INTERNATIONAL JOURNAL OF
NUMERICAL ANALYSIS AND MODELING
Volume 5, Supp , Pages 93–108

A NEW PERSPECTIVE ON TEXTURE EVOLUTION

K. BARMAK, M. EMELIANENKO, D. GOLOVATY, D. KINDERLEHRER, AND S. TA'ASAN

Abstract. Modeling and analysis of texture evolution in polycrystalline materials is a major challenge in materials science. It requires understanding grain boundary or interface evolution at the network level, where topological reconfigurations (critical events) play an important role. In this paper, we investigate grain boundary evolution in a simplified one-dimensional system designed specifically to target microstructural critical event evolution. We suggest a stochastic framework that may be used to model this system and compare predictions of the model with simulations. We discuss limitations and possible extensions of this approach to higher-dimensional cases.

Key Words. Grain boundary character, Coarsening, Texture, Continuous time random walk, Boltzmann equation.

1. Introduction

Most technologically useful materials arise as polycrystalline microstructures, composed of a myriad of small crystallites, grains separated by interfaces, grain boundaries. The energetics and connectivity of the network of boundaries are implicated in many properties across all scales of use, for example, functional properties, like conductivity in microprocessor wires, and lifetime properties, like fracture toughness in structures. Engineering a microstructure to achieve a desired set of performance characteristics is a major focus in materials science. In contemporary terms, this has led to new automated data acquisition techniques, and now we are confronted with the issue of providing accurate and predictive descriptions, theories, and models. Even though this is an important and interesting subject by itself, it is also an excellent prototype for the study of multiscale phenomena.

Of course, from a multiscale viewpoint, one may aspire to begin with a molecular description of a subset of a large granular system or cellular network, and then derive a theory for its local or mesoscale behavior, and finally pass to the macroscopic state. A special advantage in our situation is that there is a well developed local thermodynamic theory based on work of Mullins [5], Herring [2], and many others, that covers normal evolution, which is the mesoscale regime. To accomplish the passage to macroscopic level, what is frequently termed upscaling in porous media networks, we need to introduce some new quantities. Indeed, it is commonly accepted that material characteristics can be traced to statistical properties of the grain boundary network. A significant advantage of the simulation platform is our ability to alter various features to assess their role or importance in a manner more flexible than nature herself permits. Historical emphasis here has been on the geometry, or more exactly, on statistics of simple geometric features of experimental

2000 *Mathematics Subject Classification.* 60K40, 82C31, 82C40.

Research supported by grants DMS 0405343 and DMR 0520425. DG acknowledges the support of DMS 0407361 and DK acknowledges the support of DMS 0305794.

and simulated polycrystalline networks, like grain area. More recently, attention has been turned to texture, the mesoscopic description of arrangement and properties of the network described in terms of both crystallography and geometry. However, the mechanisms by which the robust distributions develop from an initial population are not yet understood. As a polycrystalline configuration coarsens, facets are interchanged, some grains grow larger, and other grains disappear. Further, when triple junctions collide, new boundaries are created. We refer to these topological rearrangements as critical events. They play an important role in the evolution of distribution functions, as we explain below. In this paper, we investigate a simplified a one-dimensional system designed specifically to target critical event evolution in microstructure and its effect on texture. We use ideas from the kinetic theory of gases to study the stochastic characteristics of a one-dimensional system of grain boundaries moving under a gradient flow. We think that this model possesses some of the main features of an interacting grain boundary network in a typical polycrystalline microstructure.

In recent years, we have witnessed the introduction of automated data acquisition technologies in the materials laboratory. This has permitted the collection of statistics on a vast scale and stands to enable an important bridge between experiments and mesoscopic simulations. There are situations, for example, where it is possible to quantify the amount of alignment or misalignment sufficient to produce a corrosion resistant microstructure [1]. To rise beyond this level of anecdotal observation, the thermodynamics of the material system must be related to texture and texture related properties. Said in a different way, are there any texture related distributions which are material properties? Some geometric features of the configuration, like relative area statistics have these properties in the sense that they are robust but they are not strongly related to energetics. Recent work has provided us with a new statistic, the grain boundary character distribution, which has enormous promise in this direction. Owing to our new ability to simulate the evolution of large scale systems, we have been able to show that this statistic is robust and, in elementary cases, easily correlated to the grain boundary energy [9]—[11].

As mentioned, the regular evolution of the network of grain boundaries in two dimensions is governed by the Mullins equations of curvature-driven growth, supplemented by the Herring condition of force balance at triple junctions—a system of parabolic equations with natural boundary conditions [12]–[7]. For the higher dimensional formulation of capillary driven growth, see [8]. When applied to a single evolving $n-$sided grain with constant grain boundary energy, this mechanism leads to the Mullins-von Neumann $n-6$ rule [3]—the rate of change of the area of the grain is proportional to $n-6$, i.e.,

$$\frac{dA_n}{dt} = \gamma(n-6) \text{ where } A_n \text{ is the area of an } n\text{-sided grain,} \tag{1}$$

and $\gamma > 0$ is some material constant. MacPherson and Srolovitz [13] have given, very recently, higher dimensional generalizations of the $n-6$ rule. In particular, from (1), grains with $3, 4$ or 5 sides decrease in area. When averaged over a population of grains, equation (1) results in

$$\frac{d\bar{A}_n}{dt} = \gamma(n-6) \text{ where } \bar{A}_n \text{ is the average area of } n\text{-sided grains.} \tag{2}$$

Inspection of Fig. 1 shows that, contrary to (2), the average area of five-sided grains in a columnar aluminum structure increases several fold over the course of

an annealing experiment. Stagnation is also present in the experiment, but this is a different matter. The $n-6$-rule does not fail for the continuous changes of boundary positions, but most of the five-sided grains we observe at time $t = 2$ hours had $6, 7, 8, ...$ sides at some earlier time $t < 2$ hours. Thus in the network setting, the critical events of grain deletion and side interchange play a major role the precise mechanism of which is not yet understood.

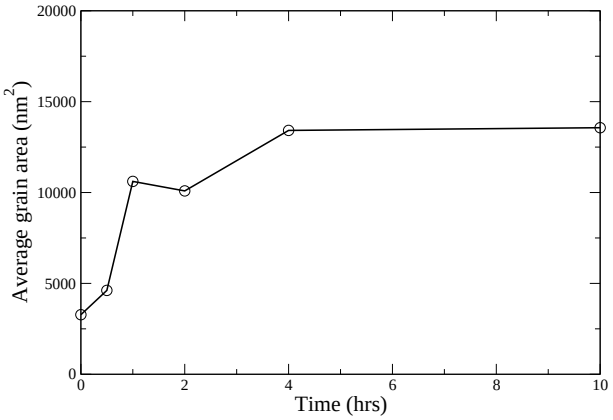

FIGURE 1. Average area of five-sided grains in an Al columnar structure.

Said differently, the grain boundary character distribution suggests that boundaries with high interfacial energies tend to shrink, while those with lower energies tend to grow. On the other hand, in a system with only geometric evolution, a grain grows or shrinks depending on its number of sides. These two situations represent extremes of behavior and in reality both effects should be taken into account. Impressive computational results have been obtained recently by [14] for a type of a birth-death model in the case of a sharp Read-Schockley type of grain boundary energy potential.

To gain an insight into the influence of critical events on the coarsening dynamics, here we model the evolution of statistical characteristics of a relatively simple, one-dimensional system of grain boundaries. The model preserves features of an interacting grain boundary network—boundaries and junctions between boundaries moving under a form of a gradient flow.

The one-dimensional model was introduced in [17] and [18] to investigate the critical events that occur during interface evolution. In particular, we used probabilistic arguments to develop a statistical model for critical events and investigated the applicability of a fractional continuous time random walk theory. Even though the fractional random walk dynamics appears to be appropriate for approximating some intermediate regimes in the evolution of the grain boundary system, the "slowing-down" coarsening effects require a more general stochastic framework. A possible approach identified in [18] is based on identifying the stochastic features of the system and formulating and solving the appropriate master equation.

In this paper we introduce an alternative framework based on a statistical mechanics approach (Section 4). To describe the evolution of statistical characteristics

of the one-dimensional system of grain boundaries, we propose two kinetic models that differ in their choice of the underlying phase space (the type and the number of state variables needed to describe an individual boundary). Both models lead to a Boltzmann-type equation for a number density of states. The numerical solution of these equations qualitatively reproduce the distributions obtained via simulation of the deterministic system of grain boundaries. Not unexpectedly, the quantitative predictions of the equation based on a larger state space are more accurate but also computationally more expensive.

2. One-dimensional model

Our principal goal is to understand whether it is possible to derive a stochastic model of grain growth by conducting numerical experiments for a large number of evolving grains, collecting the appropriate statistical data, and using this data to formulate a mathematical model governing the evolution of relevant effective characteristics. In this paper, we demonstrate the feasibility of this approach by introducing a one-dimensional system of grain boundaries represented by intervals on a number line. Note that we do not claim that such a system is physically realistic—there is no curvature-driven propagation in one dimension. Rather, our interest is in studying the dynamics of a system where interactions between grain boundaries resemble qualitatively those observed in a real polycrystalline material. We assume that each grain boundary is described by its length and a prescribed "orientation". We require that there are only nearest-neighbor interactions between the grain boundaries and that the strength of the interactions depends on values of the orientation parameter for the neighboring boundaries.

To make our system precise, fix $L > 0$ and consider the intervals $[x_i, x_{i+1}]$, $i = 0, \dots, n-1$ on the real line where $x_i \leq x_{i+1},\ i = 0, \dots, n-1$ and $x_n = x_0 + L$. The locations of the endpoints $x_i,\ i = 0, \dots, n$ may vary in time and the total length L of all intervals remains fixed. For each interval $[x_i, x_{i+1}]$, $i = 0, \dots, n-1$, choose a number α_i from the set $\{\alpha_j\}_{j=1,\dots,n}$. The intervals $[x_i, x_{i+1}]$ correspond to grain boundaries and the points x_i represent the triple junctions. The parameters $\{\alpha_i\}_{i=1,\dots,n}$ can be viewed as representing crystallographic *orientations*. The *length* of the i^{th} grain boundary is given by $l_i = x_{i+1} - x_i$. Now choose a non-negative energy density $f(\alpha)$ and define the energy

$$En(t) = \sum f(\alpha_i)(x_{i+1}(t) - x_i(t)) \tag{3}$$

Consider gradient flow dynamics characterized by the system of ordinary differential equations

$$\dot{x}_i = f(\alpha_i) - f(\alpha_{i-1}),\ i = 0, \dots, n. \tag{4}$$

The parameter α_i is prescribed for each grain boundary initially according to some random distribution and does not change during its lifetime. The *velocities* of the grain boundaries can be computed from the relation

$$v_i = \dot{x}_{i+1} - \dot{x}_i = f(\alpha_{i+1}) + f(\alpha_{i-1}) - 2f(\alpha_i). \tag{5}$$

Notice that the velocities remain constant until the moment of a *critical event* when a neighboring grain boundary collapses, at which instant a jump of the velocity occurs. Every critical event changes the statistical state of the model through its effect on the grain boundary velocities and, therefore, affects further evolution of the grains. Notice that the lengths of the individual grain boundaries vary linearly with time between the corresponding jump events with the rate that depends entirely on the corresponding grain boundary velocities.

An important feature of the thermodynamics of grain growth is that it is dissipative for the energy during normal grain growth, [12]. At critical events, the algorithm (4) is designed to enforce dissipation. To verify that (4) is dissipative, first consider a time t between two critical events. Then

$$\begin{aligned}\frac{dEn}{dt}(t) &= \sum f(\alpha_i)v_i = \sum f(\alpha_i)(f(\alpha_{i+1}) + f(\alpha_{i-1}) - 2f(\alpha_i)) \\ &\leqq 2\Big(\sum f(\alpha_i)^2\Big)^{\frac{1}{2}}\Big(\sum f(\alpha_i)^2\Big)^{\frac{1}{2}} - 2\sum f(\alpha_i)^2 = 0\end{aligned}$$

by periodicity and the Schwarz Inequality. This also corresponds to the fact that for any gradient flow dynamics

$$(\dot{x}_i)^2 = -\frac{\partial En}{\partial x_i}\dot{x}_i, \tag{6}$$

so that

$$\frac{\partial En}{\partial t} = -\sum \dot{x}_i^2 < 0. \tag{7}$$

Now suppose that the grain boundary $[x_c, x_{c+1}]$ vanishes at time $t = t_c$ and it is the only grain boundary vanishing at t_c. Then the velocity of that boundary $v_c(t) < 0,\ t < t_c$, namely,

$$\frac{1}{2}(f(\alpha_{c+1}) + f(\alpha_{c-1})) < f(\alpha_c). \tag{8}$$

and $l_c \to 0$ for $t \to t_c^-$. Now

$$En(t) > \sum_{i\neq c} f(\alpha_i)l_i,\ t < t_{crit}, \tag{9}$$

and

$$En(t_{crit}) = \lim_{t\to t_{crit}} \sum_{i\neq c} f(\alpha_i)l_i \leqq \lim_{t\to t_{crit}} En(t). \tag{10}$$

Thus the model system is dissipative.

From the materials science perspective, it is important to know both the distributions of relative lengths, as well as the grain orientations. In the most general case, we have a state space $S = \{(l, v, \alpha)\}$, where $l \in \mathbb{R}^+$, $v \in \mathbb{R}$, and $\alpha \in (a, b)$.

Our goal is to obtain (if possible) a set of equations describing time evolution of the joint probability density function (pdf) $\rho(l, v, \alpha, t)$ and, therefore, the effective dynamics of the deterministic one-dimensional grain growth model associated with (4).

3. Simulation statistics

As a first step toward a mesoscopic model we identify the set of stable statistics by simulating the one-dimensional system that evolves according to (5). The statistics of several numerical experiments for a system of 10000 grain boundaries is presented in Figures 2 and 3. Note that, unless there are coincident events, 10000 grain boundaries disappear exactly after 10000 critical events.

Figure 2 shows evolution of the relative area and the relative velocity distributions for the case of a single-well potential (the distributions are similar for other choices of f and, indeed, resemble the two dimensional statistics reported in [11]). Both statistics do not change their overall shape in the later part of the simulation, however, their spread narrows with time because fewer and fewer grain boundaries remain in the system. If the axes are scaled accordingly, we observe the stabilization of both distributions (Figure 2).

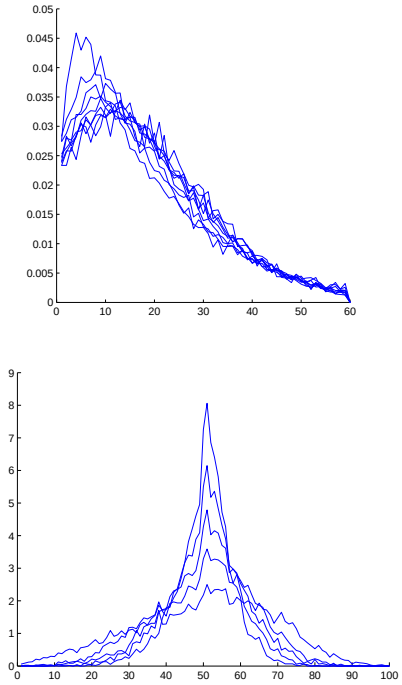

FIGURE 2. Evolution of marginal probability density functions for: (a) relative length, (b) relative velocities when $f = (x - 0.5)^2$

In the Figure 3 we present the distributions for the orientation parameters α when f has either one or two minima. The graphs clearly show that the shapes of f and orientations distribution are inversely correlated.

4. Boltzmann-type kinetic equation

4.1. Grain boundary network as a network of interacting particles. Adopting a statistical mechanics [20], [19] perspective, we will regard the system of grain boundaries as a collection of interacting "particles", where the state of each particle is determined by the parameters of the corresponding boundary. Some of these parameters—such as the length l—vary continuously with time and some—such as the orientation α and the velocity v—can change only when a grain boundary disappears during a critical event. From now on, exploiting the grain-boundary/particle analogy, we will also refer to the critical events as "collisions". Note that exactly three grain boundaries are involved in each collision—one boundary disappears while two of its immediate neighbors come in contact.

We will use the following set of conventions in order to distinguish between various types of colliding grain boundaries (Figure 4):

(1) The parameters of a grain boundary that exists prior to and is involved in a collision will carry an asterisk, i.e. (l^*, v^*, α^*).
(2) For every $i, j \in \mathbf{N}$, the subscripts $(+i)$ and $(-j)$ will be used, respectively, to label the parameters of the i-th right and the j-th left neighbor of a given grain boundary.

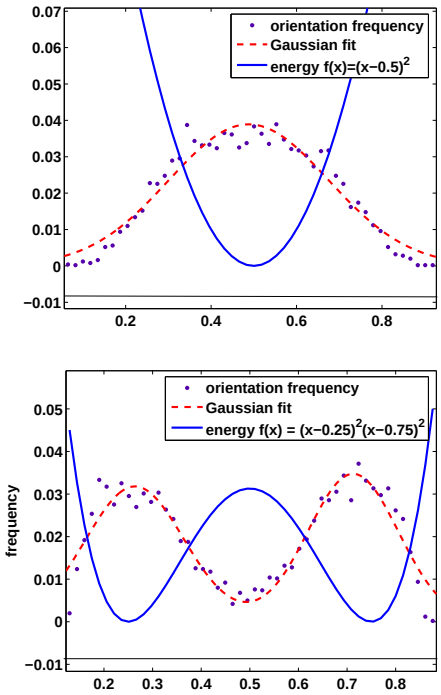

FIGURE 3. Probability density functions of the orientation parameter α for the two different choice of energy density. (a) $f(x) = (x-0.5)^2$, (b) $f(x) = (x-0.5)^2(x-1)^2(x-1.5)^2$.

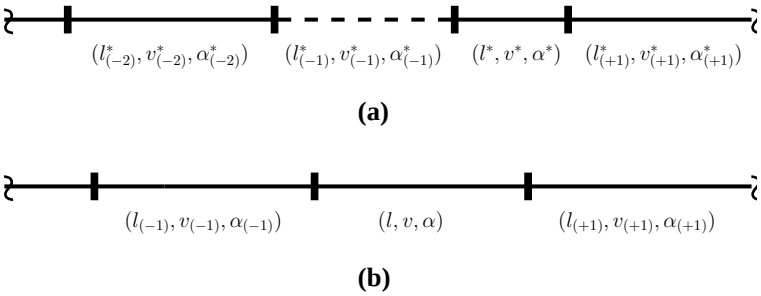

FIGURE 4. Labeling of the grain boundaries (a) before and (b) after a collision. The disappearing boundary is represented by the dashed line.

We will make extensive use of the relationship (5) which can be written as

$$v = f\left(\alpha_{(-1)}\right) + f\left(\alpha_{(+1)}\right) - 2f(\alpha), \tag{11}$$

in the new notation.

In what follows, we will consider two possible choices of a phase space for the one-dimensional grain boundary system: we will assume that a grain boundary is characterized by a set of either three (l, v, α) (model A) or four $(l, \alpha_{(-1)}, \alpha, \alpha_{(+1)})$ (model B) variables. Observe that the lower-dimensional phase space formulation

possibly carries less information about the state of the grain boundary network, but may lead to a computationally less expensive model.

4.2. Model A.

4.2.1. Collision rules. In order to formulate the appropriate kinetic equations we need to define the collision rules that relate the parameters of the new grain boundaries that form in collisions.

Suppose that the length of the first neighbor to the left of a boundary (l^*, v^*, α^*) shrinks to zero at a time t. According to (11) the following relationships hold immediately before the collision

$$v^* = f\left(\alpha^*_{(+1)}\right) + f\left(\alpha^*_{(-1)}\right) - 2f(\alpha^*), \tag{12}$$

$$v^*_{(-1)} = f\left(\alpha^*\right) + f\left(\alpha^*_{(-2)}\right) - 2f\left(\alpha^*_{(-1)}\right). \tag{13}$$

At the time of the collision, the grain boundary $\left(0, v^*_{(-1)}, \alpha^*_{(-1)}\right)$ disappears and the boundaries (l^*, v^*, α^*) and $\left(l^*_{(-2)}, v^*_{(-2)}, \alpha^*_{(-2)}\right)$ come in contact to form the two new grain boundaries, (l, v, α) and $\left(l_{(-1)}, v_{(-1)}, \alpha_{(-1)}\right)$. Both the lengths and the orientations of the boundaries that have existed prior to the collision, transfer without change to those of new boundaries, in particular,

$$\alpha = \alpha^*,\ l = l^*,\ \alpha_{(-1)} = \alpha^*_{(-2)}. \tag{14}$$

The velocity of the boundary (l, v, α) that replaces (l^*, v^*, α^*) can be determined from (11) and is given by

$$v = f(\alpha_{(-1)}) + f(\alpha_{(+1)}) - 2f(\alpha). \tag{15}$$

From (12)-(15) we obtain the relationship

$$v = v^* + v^*_{(-1)} + f\left(\alpha^*_{(-1)}\right) - f(\alpha), \tag{16}$$

between the velocity v of the new grain boundary and the parameters of the two boundaries—$\left(0, v^*_{(-1)}, \alpha^*_{(-1)}\right)$ and (l^*, v^*, α^*)—that have collided at the time t. The first two equations in (14) and the equation (16) can be interpreted as the closed set of "collision" rules that define the grain boundary (l, v, α) in terms of parameters of its colliding "parent" boundaries $\left(0, v^*_{(-1)}, \alpha^*_{(-1)}\right)$ and (l^*, v^*, α^*). Note that this kind of collision dynamics resembles the "sticky" collisions of completely inelastic particles observed, for example, in granular gases [21].

Without loss of generality, we assume that the potential f satisfies $\min f = 0$. By (11), we have for any grain boundary (l, v, α) that

$$v + 2f(\alpha) = f(\alpha_{(-1)}) + f(\alpha_{(+1)}) \geq 0.$$

The admissible set in the phase space is given by

$$\mathcal{A} := \{(l, v, \alpha) \mid l \geq 0,\ v + 2f(\alpha) \geq 0\}. \tag{17}$$

When $\left(0, v^*_{(-1)}, \alpha^*_{(-1)}\right)$ collides from the left with (l^*, v^*, α^*) to form (l, v, α), the equations (12)-(14) provide the following constraints on the parameters of the colliding boundaries

$$\begin{cases} v^* + 2f(\alpha) - f\left(\alpha^*_{(-1)}\right) = f\left(\alpha^*_{(+1)}\right) \geq 0, \\ v^*_{(-1)} + 2f\left(\alpha^*_{(-1)}\right) - f\left(\alpha\right) = f\left(\alpha^*_{(-2)}\right) \geq 0. \end{cases} \tag{18}$$

By (15) and (18) the new boundary (l, v, α) satisfies $v+2f(\alpha) \geq 0$, thus $(l, v, \alpha) \in \mathcal{A}$.

By eliminating v^* from the first inequality in (18) and using (16), we find that $v^*_{(-1)}+2f\left(\alpha^*_{(-1)}\right) \leq v+3f(\alpha)$. Combining this inequality with the second inequality in (18) we obtain the set of constraints

$$f(\alpha) \leq v^*_{(-1)} + 2f\left(\alpha^*_{(-1)}\right) \leq v + 3f(\alpha), \tag{19}$$

on the admissible values of the parameters of a grain boundary the collision of which from the left with another grain boundary would result in formation of a grain boundary residing in the state (l, v, α).

The dynamics of a density of states in the phase space is determined by the continuous evolution of lengths between the collision events and discrete changes in velocities and orientations during these events. Next we formulate the equation that describes the evolution of the density function.

4.2.2. Evolution equation. Let $N(t)$ be the number of grain boundaries in the system at time t and set $N_0 := N(0)$. Note that the function N is non-increasing. Now suppose that $\rho(l, v, \alpha, t)$ represents the number density of states of the grain boundary system at a time t and satisfies

$$\int_{\mathcal{A}} \rho(l, v, \alpha, t)\, dl\, dv\, d\alpha = N(t), \tag{20}$$

that is $N_0^{-1}\rho(l, v, \alpha, t)dl\, dv\, d\alpha$ is a fraction of the initial number of the grain boundaries that are still present in an element $[l, l + dl] \times [v, v + dv] \times [\alpha, \alpha + d\alpha]$ of the phase space at the time t.

Since we interpret collisions as occurring between two boundaries one of which shrinks to a point at the time of the collision, we will simplify the notation by labeling the shrinking boundary as $(0, v', \alpha')$ as shown in Figure 5.

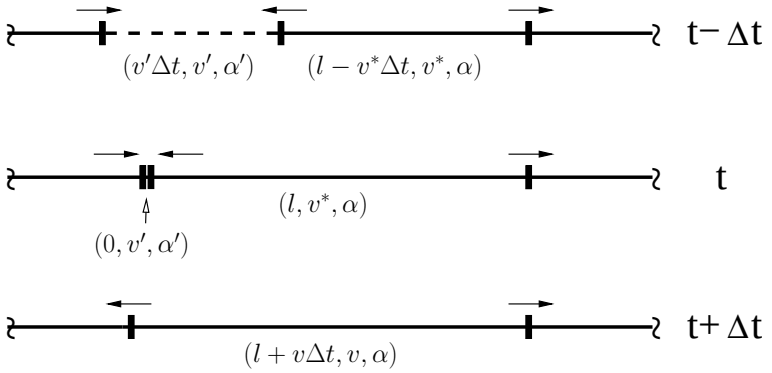

FIGURE 5. Schematic of a collision event. For each junction between the boundaries, the arrow indicates the direction of motion. The velocity $v = v^* + v' + f(\alpha') - f(\alpha)$ by (16).

Then, using (16), (19), and the fact that the grain boundaries may disappear with equal probability both to the left and to the right of a given boundary, we find that the rate per unit volume of the phase space at which the boundaries are created in $[l, l + dl] \times [v, v + dv] \times [\alpha, \alpha + d\alpha]$ is given by

$$W_+ := -\frac{1}{N(t)} \int_{A_+} v' \rho\,(0, v', \alpha', t)\, \rho\,(l, v - v' + f(\alpha) - f(\alpha'), \alpha, t)\; d\alpha' dv', \tag{21}$$

where $A_+ := \{f(\alpha) \le v' + 2f(\alpha') \le v + 3f(\alpha)\} \cap \{v' < 0\}$. Here the second restriction on the domain of integration is due to the requirement that v' must be negative to ensure that (l', v', α') is shrinking.

Now suppose that the grain boundaries $(0, v', \alpha')$ and (l, v, α) collide to form the boundary (l, w, α), where

$$w = v + v' + f(\alpha') - f(\alpha), \tag{22}$$

(cf. (16)). The collision is feasible if

$$\begin{cases} v' + 2f(\alpha') - f(\alpha) \ge 0, \\ v + 2f(\alpha) - f(\alpha') \ge 0, \end{cases} \tag{23}$$

(cf. (18)) and $(0, v', \alpha')$ must satisfy the constraints

$$v' + 2f(\alpha') \ge f(\alpha), \;\; f(\alpha') \le v + 2f(\alpha). \tag{24}$$

Then the rate per unit volume of the phase space at which the boundaries are removed from the element $[l, l + dl] \times [v, v + dv] \times [\alpha, \alpha + d\alpha]$ is given by

$$W_- := -\frac{1}{N(t)} \int_{A_-} v' \rho(0, v', \alpha', t) \rho(l, v, \alpha, t)\, d\alpha' dv', \tag{25}$$

where $A_- := \{f(\alpha) \le v' + 2f(\alpha')\} \cap \{f(\alpha') \le v + 2f(\alpha)\} \cap \{v' < 0\}$.

By taking into account the flux across the boundary of the element of the phase space (due to continuous dependence of lengths of the grain boundaries on time), we arrive at the following form of the kinetic equation

$$\frac{\partial \rho(l, v, \alpha, t)}{\partial t} + v \frac{\partial \rho(l, v, \alpha, t)}{\partial l} = W. \tag{26}$$

Here the term on the right hand side accounts for the changes in the population due to collisions

$$W := W_+ - W_- = \{gain\} - \{loss\}. \tag{27}$$

Then

$$\begin{aligned} &\frac{\partial \rho(l, v, \alpha, t)}{\partial t} + v \frac{\partial \rho(l, v, \alpha, t)}{\partial l} = \\ &-\frac{1}{N(t)} \int_{A_+} v' \rho(0, v', \alpha', t) \rho(l, v - v' + f(\alpha) - f(\alpha'), \alpha, t)\, d\alpha' dv' \\ &+\frac{1}{N(t)} \int_{A_-} v' \rho(0, v', \alpha', t) \rho(l, v, \alpha, t)\, d\alpha' dv'. \end{aligned} \tag{28}$$

This evolution equation has been simulated and produced reasonable results when compared to the microscopic dynamics, as shown later in Section 5. The major obstacle in using this approach lies in the increased computational complexity associated with evaluating double integrals in (28).

4.3. Model B. Here we assume that the state of a grain boundary is given by four parameters $(l, \alpha_{(-1)}, \alpha, \alpha_{(+1)})$. Although the phase space is larger in this case, the collision rules are simpler than those for the model A. Indeed, the velocity of both the boundary and the junctions with its neighbors to the right and to the left can be uniquely determined via (11) and (4), respectively.

Set $\mathcal{B} := \mathbf{R}_+ \times \mathbf{R}^3$. Suppose that a grain boundary $\big(0, \beta_{(-1)}, \beta, \beta_{(+1)}\big) \in \mathcal{B}$ disappears to the left of the grain boundary $\big(l, \alpha_{(-1)}, \alpha, \alpha_{(+1)}\big) \in \mathcal{B}$ (Figure 6). Clearly, $\beta = \alpha_{(-1)}$ and $\beta_{(+1)} = \alpha$. Further, the collision leads to the formation of the new boundary $\big(l, \beta_{(-1)}, \alpha, \alpha_{(+1)}\big) \in \mathcal{B}$.

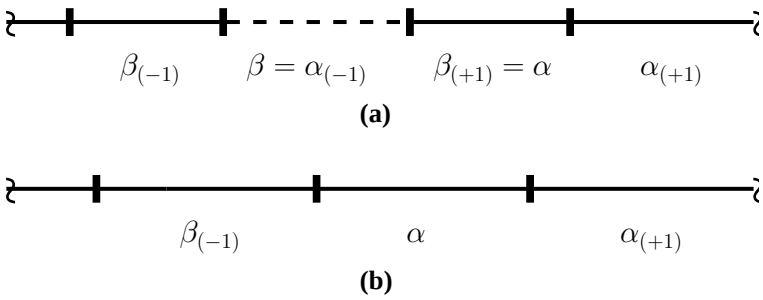

FIGURE 6. Orientations of the grain boundaries (a) before and (b) after a collision. The disappearing boundary is represented by the dashed line.

As before, let $N(t)$ be the number of grain boundaries in the system at time t, denote $N_0 := N(0)$, and suppose that $\rho\left(l, \alpha_{(-1)}, \alpha, \alpha_{(+1)}, t\right)$ represents the number density of states of the grain boundary system at a time t. Then ρ satisfies

$$\int_{\mathcal{B}} \rho\left(l, \alpha_{(-1)}, \alpha, \alpha_{(+1)}, t\right)\, dl\, d\alpha\, d\alpha_{(-1)}\, d\alpha_{(+1)} = N(t). \tag{29}$$

Further, we assume that $\rho(l, x, y, z, t) = \rho(l, z, y, x, t)$ for every $(l, z, y, x) \in \mathcal{B}$ and $t \geq 0$.

The rate at which the grain boundaries are added to an element of the phase space $[l, l+dl] \times \left[\alpha_{(-1)}, \alpha_{(-1)} + d\alpha_{(-1)}\right] \times [\alpha, \alpha + d\alpha] \times \left[\alpha, \alpha_{(+1)} + d\alpha_{(+1)}\right]$ is given by

$$\begin{aligned} W_+ &:= \tfrac{1}{N(t)} \textstyle\int_{\mathcal{B}} \left(2f(s) - f(\alpha) - f(\alpha_{(-1)})\right) \rho\left(0, \alpha_{(-1)}, s, \alpha\right) \rho\left(l, s, \alpha, \alpha_{(+1)}\right)\, ds \\ &+ \tfrac{1}{N(t)} \textstyle\int_{\mathcal{B}} \left(2f(s) - f(\alpha) - f(\alpha_{(+1)})\right) \rho\left(0, \alpha, s, \alpha_{(+1)}\right) \rho\left(l, \alpha_{(-1)}, \alpha, s\right)\, ds. \end{aligned} \tag{30}$$

Similarly

$$\begin{aligned} W_- &:= \tfrac{1}{N(t)} \textstyle\int_{\mathcal{B}} \left(f(\alpha) + f(s) - 2f(\alpha_{(-1)})\right) \rho\left(0, s, \alpha_{(-1)}, \alpha\right) \rho\left(l, \alpha_{(-1)}, \alpha, \alpha_{(+1)}\right)\, ds \\ &+ \tfrac{1}{N(t)} \textstyle\int_{\mathcal{B}} \left(f(\alpha) + f(s) - 2f(\alpha_{(+1)})\right) \rho\left(0, \alpha, \alpha_{(+1)}, s\right) \rho\left(l, \alpha_{(-1)}, \alpha, \alpha_{(+1)}\right)\, ds. \end{aligned} \tag{31}$$

The kinetic equation has the following form

$$\begin{aligned} &\frac{\partial \rho\left(l, \alpha_{(-1)}, \alpha, \alpha_{(+1)}\right)}{\partial t} \\ &+ \left(f\left(\alpha_{(-1)}\right) + f\left(\alpha_{(+1)}\right) - 2f(\alpha)\right) \frac{\partial \rho\left(l, \alpha_{(-1)}, \alpha, \alpha_{(+1)}\right)}{\partial l} = W, \end{aligned} \tag{32}$$

where the collision integral $W = W_+ - W_-$ and W_+ and W_- are given by (30)-(31).

5. Numerical results

Here we find the numerical solutions of the equations (28) and (32) and compare the results with those obtained by simulating the deterministic one-dimensional system of grain boundaries.

We begin by describing the numerical procedure for the model A—the procedure is the same for model B (with minor modifications). First, we construct the initial condition for the number density of states. We fix the initial number of grain boundaries in the system to be $n = 10000$ and supply each model with a random

input data in the form of n orientation parameters α and n randomly distributed lengths of the boundaries l. Velocities are then computed by the rules given in (4).

Note that the region occupied by the system in the phase space continuously grows with time in the l-direction. In order to keep the numerical procedure simple and the size of the simulation small, we introduce an artificial constraint on a grain boundary length by assuming that l cannot exceed some (relatively large) $L > 0$. The drawback of imposing this constraint is that the accuracy of the simulation will be affected for large times when the system can grow beyond the computational domain.

Next we discretize the domain $\Omega := [0, L] \times [-1, 1] \times [0, 2]$ in the phase space by using a uniform mesh with $n_\alpha = n_v = 20$ and $n_l = 100$ discretization points in the α-, v-, and l-directions, respectively. Each cell of this discretization also serves as a "bin" containing some states of the randomly generated data; by counting the number of states in each bin we obtain the initial condition on the number density of states.

We discretize equation (28) by using an explicit upwind scheme in which the spatial derivative is discretized as $v\frac{\partial \rho}{\partial l}(l, v, \alpha, t) \sim \frac{v}{2}(\rho(l+dl, v, \alpha, t) - \rho(l-dl, v, \alpha, t)) - \frac{|v|}{2}(\rho(l + dl, v, \alpha, t) - 2\rho(l, v, \alpha, t) + \rho(l - dl, v, \alpha, t))/dl$ for all interior points of Ω; we use a forward difference scheme for the boundary $l = 0$ and a backward difference scheme for the boundary $l = L$. The collision integral is then computed by calculating lower-right Riemann sums for the admissible pairs of (v, α) as specified by the sets A_- and A_+.

In Figures 7-9 we present the results of the numerical experiments. For three different choices of the energy functional, we compare the statistics obtained via simulations of the deterministic system with those obtained by numerically solving the equation (28) of model A.

Although a very good agreement exists for the distributions of both lengths and orientations, the deviation between the corresponding distributions of the velocities becomes significant after some time. There are several factors that can contribute to such behavior. Some factors may be numerical in nature (e.g. there are discretization errors), some may be due to the modeling assumptions that are too restrictive (the development of correlations that are not accounted for in the model), and some may be inherent to the inevitable loss of information when passing from the deterministic to the effective kinetic model (Boltzmann equation does not conserve the total length of all grain boundaries in the system, the number of state variables may be too small, etc.).

The results obtained using the model B agree very well with the deterministic simulations for all times for which the simulations were performed (Figure 10). A drawback of the Model B as compared to the model A, is that the equation (32) requires more variables. While this may not be an issue in the one-dimensional example considered here, there may be significant differences between the two models in the computational power needed to describe grain boundaries in the real two- or three-dimensional systems.

6. Discussion

In this work, we have presented a new framework for modeling critical events in microstructure evolution and analyzed its capabilities by applying it to a simplified model, originally introduced in [17]. The model is specifically designed to target the evolution of triple junctions during grain growth disregarding mean curvature effects present in the real systems. In [17], [18], we analyzed the stochastic properties of

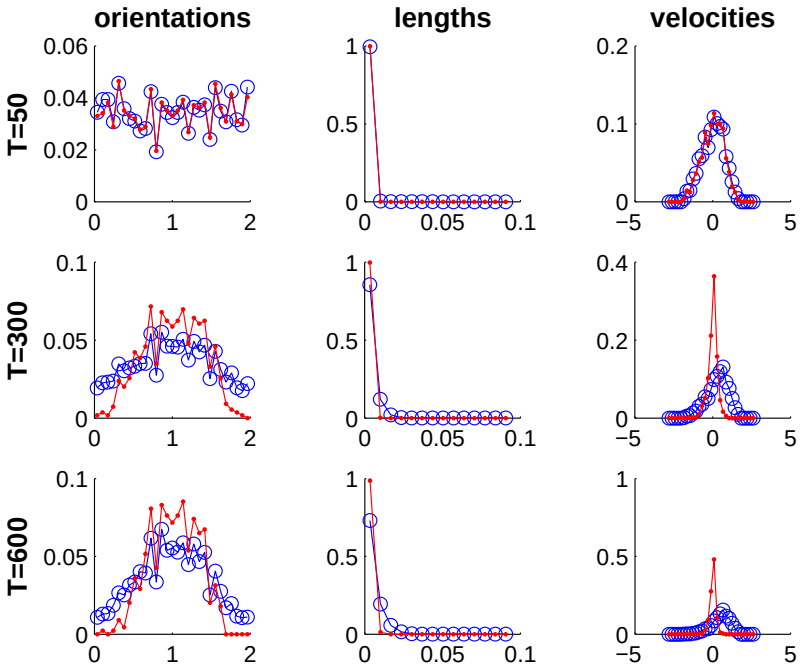

FIGURE 7. Model A. Comparison of the marginal distributions for orientations (left), lengths (center), and velocities (right) when the energy function is given by $f(x) = (x-1)^2$. The deterministic simulations and the solution of the Boltzmann equation (28) are plotted using points and circles, respectively.

this system and discovered that despite its simplicity it exhibits a wide range of complex nonlinear dynamics phenomena, from fractional diffusion to non-identically distributed waiting times. While we have been able to successfully describe some stages of the evolution by means of the random walk theory, the search for a unified and computationally feasible statistical theory is not over. Here we focused on an alternative approach which offers some advantages in describing parts of the system evolution and helps explain some of the stochastic phenomena observed in previous work.

This approach is motivated by the theory of sticky particle dynamics. It has a capability to model critical events more thoroughly through the set of collision rules and hence goes beyond the averaging ideas. The approach proved to be effective in the early stages of the simulation for the model A based on a smaller number of state variables. For larger times, the discrepancy between the kinetic model A and its deterministic counterpart becomes larger. A possible remedy, proposed in this work, is to consider a larger state space kinetic model (model B). The corresponding Boltzmann equation takes into account all local reconfigurations in the grain boundary network and successfully reproduces the distributions during full system lifecycle. This approach, however, may require a significantly larger computations for the higher dimensional problems.

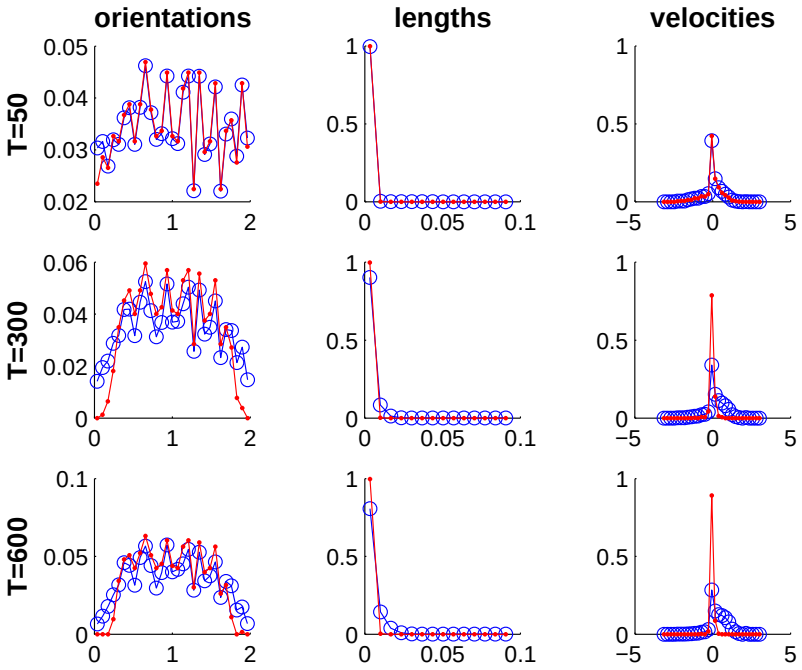

FIGURE 8. Model A. Comparison of the marginal distributions for orientations (left), lengths (center), and velocities (right) when the energy function is given by $f(x) = (x - 0.5)^2(x - 1)^2(x - 1.5)^2$. The deterministic simulations and the solution of the Boltzmann equation (28) are plotted using points and circles, respectively.

7. Acknowledgment

The authors wish to thank their colleagues Eva Eggeling, Gregory Rohrer, and A. D. Rollett.

References

[1] E. M. Lehockey, G. Palumbo, P. Lin, and A. Brennenstuhl. Mitigating intergranular attack and growth in lead-acid battery electrodes for extended cycle and operating life, Metall. Mater. Trans., A Phys. Metall. Mater. Sci., 29 (1998) 7–117.

[2] C. Herring, Surface tension as a motivation for sintering, in The Physics of Powder Metallurgy, W.E. Kingston, ed., MacGraw Hill, New York, (1951), 142-179

[3] Mullins, W. W., A One Dimensional Nearest Neighbor Model of Coarsening, Proceedings of the Calculus of Variations and Nonlinear Material Behavior, Carnegie Mellon University, 1990

[4] Mullins, W.W., Two-dimensional Motion of Idealized Grain Boundaries, J. Appl. Phys., 27 (1956) 900–904.

[5] Mullins, W.W., *Solid Surface Morphologies Governed by Capillarity*, In Metal Surfaces: Structure, Energetics, and Kinetics, ASM, Cleveland, 1963

[6] S. Agmon, A. Douglis and L. Nirenberg, Estimates near the boundary for solutions of elliptic partial differential equations satisfying general boundary conditions, II, Comm. Pure Appl. Math. 17 (1964) 35–92.

[7] L. Bronsard and F. Reitich, On three-phase boundary motion and the singular limit of a vector-valued Ginzburg-Landau equation, Arch. Rat. Mech. Anal. 124 (1993) 355–379.

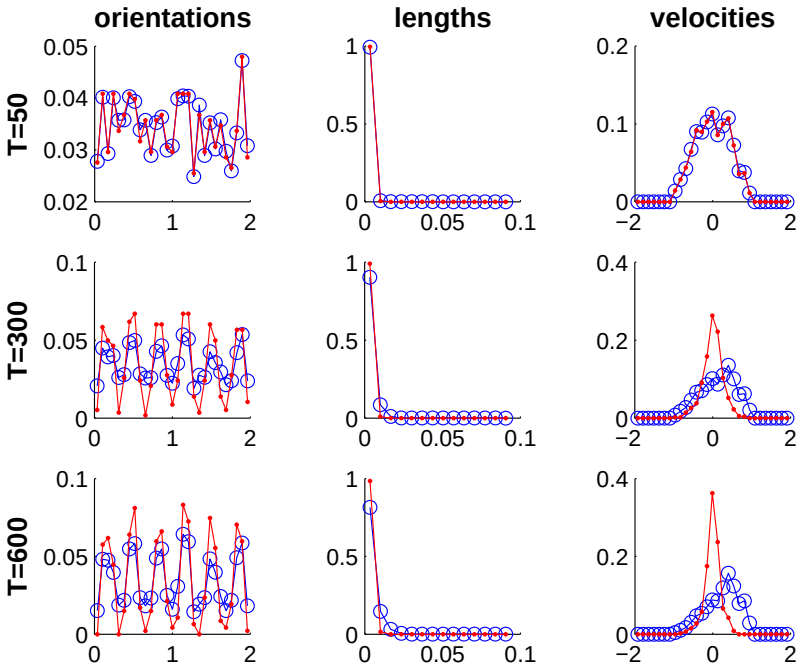

FIGURE 9. Model A. Comparison of the marginal distributions for orientations (left), lengths (center), and velocities (right) when the energy function is given by $f(x) = (\cos(6x\pi) + 1)/4$. The deterministic simulations and the solution of the Boltzmann (28) equation are plotted using points and circles, respectively.

[8] D. Kinderlehrer, J. Lee, I. Livshits, and S. Ta'asan. *Mesoscale simulation of grain growth.* In Continuum Scale Simulation of Engineering Materials(Raabe, D. et al., eds), pages 361–372, Wiley-VCH Verlag, Weinheim, 2004.

[9] D. Kinderlehrer, I. Livshits, G. S. Rohrer, S. Ta'asan, and P. Yu, Mesoscale evolution of the grain boundary character distribution. Recrystallization and Grain Growth, Materials Science Forum 467-470 (2004) 1063–1068.

[10] D. Kinderlehrer, I. Livshits, F. Manolache, G. S. Rohrer, S. Ta'asan, *An approach to the mesoscale simulation of grain growth* In Influences of interface and dislocation behavior on microstructure evolution (Aindow, M. et al., eds), Mat. Res. Soc. Symp. Proc. 652, Y1.5., 2001.

[11] D. Kinderlehrer, I. Livshits, and S. Ta'asan, A variational approach to modeling and simulation of grain growth, SIAM J. Sci. Comput., 28 (2006) 1694–1715.

[12] D. Kinderlehrer and C. Liu, Evolution of grain boundaries, Math. Models and Meth. Appl. Math., 11.4 (2001) 713–729.

[13] R. D. MacPherson and D. J. Srolovitz, The von Neumann relation generalized to coarsening of three-dimensional microstructures, Nature, 446 (2007) 1053–1055.

[14] J. Gruber, thesis, CMU 2007, cf. also G.S. Rohrer, Influence of Interface Anisotropy on Grain Growth and Coarsening," Annual Review of Materials Research 35 (2005) 99-126

[15] V.E. Fradkov, D. Udler, Two-dimensional normal grain growth: topological aspects, Advances in Physics, 43 (1994) 739–789.

[16] H.V.Atkinson, Theories on normal grain growth in pure single phase systems, Acta Metall., 36 (1988) 469–491.

[17] M. Emelianenko, D. Golovaty, D. Kinderlehrer, and S. Taasan, Toward a statistical theory of texture, submitted to SIAM J. Sci. Comput., 2007.

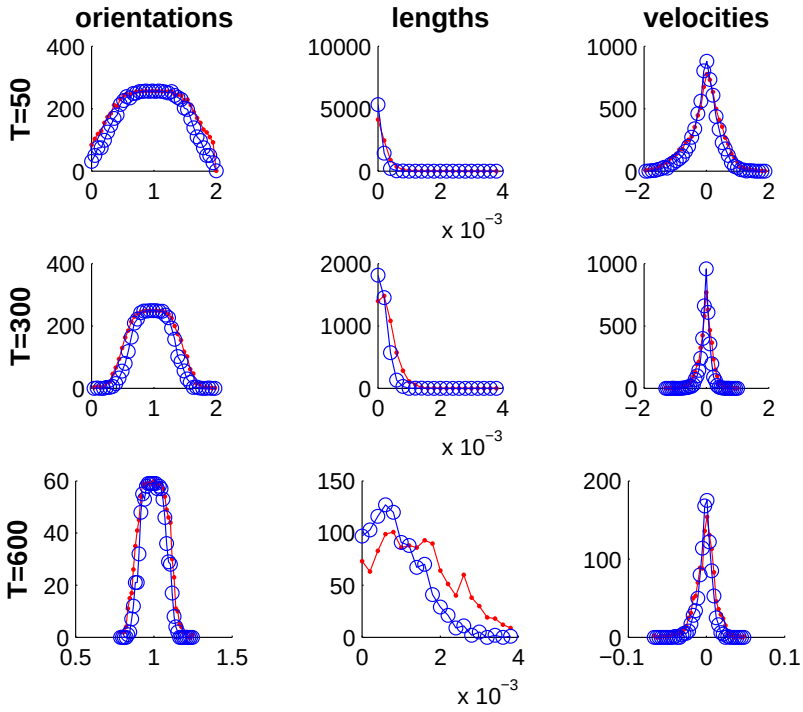

FIGURE 10. Model B. Comparison of the marginal distributions for orientations (left), lengths (center), and velocities (right) when the energy function is given by $f(x) = (x-0.5)^2$. The deterministic simulations and the solution of the Boltzmann equation (32) are plotted using points and circles, respectively.

[18] K. Barmak, M. Emelianenko, D. Golovaty, D. Kinderlehrer, and S. Taasan., *On a statistical theory of critical events in microstructural evolution*, in proceedings of 11th International Symposium on Continuum Models and Discrete Systems, Paris, 30 July - 3 August, 2007 (CMDS11), 2007

[19] Anna de Masi, Enrico Presutti, Mathematical Methods for Hydrodynamic Limits, Springer-Verlag, 1991

[20] Ludwig Boltzmann, Lectures on gas theory, Dover, 1995

[21] D. Benedetto, E. Caglioti, M. Pulvirenti, A kinetic equation for granular media, Math. Mod. and Num. An., 31 (1997) 615–641.

Department of Materials Science and Engineering, Carnegie Mellon University, Pittsburgh, PA 15213

E-mail: katayun@andrew.cmu.edu

Department of Mathematical Sciences, George Mason University, Fairfax, VA 22030

E-mail: memelian@gmu.edu

Department of Theoretical and Applied Mathematics, The University of Akron, Akron, OH 44325

E-mail: dmitry@math.uakron.edu

Department of Mathematical Sciences, Carnegie Mellon University, Pittsburgh, PA 15213

E-mail: davidk@cmu.edu and shlomo@andrew.cmu.edu